THE ASTROPHYSICAL JOURNAL, 365:681–685, 1990 December 20

RADIO AND X-RAY STATES IN THE X-RAY BINARY SCORPIUS X-1

R. M. HJELLMING
National Radio Astronomy Observatory,[1] Socorro
R. T. STEWART AND G. L. WHITE
CSIRO, Division of Radiophysics
R. STROM
Netherlands Foundation for Research in Astronomy, Radiosterrenwacht
W. H. G. LEWIN
Center for Space Research, Cambridge
P. HERTZ, K. S. WOOD, AND J. P. NORRIS
E. O. Hulburt Center for Space Astronomy, Naval Research Laboratory
K. MITSUDA
Institute of Space and Astronautical Science
AND
W. PENNINX AND J. VAN PARADIJS
Astronomical Institute "Anton Pannekoek," University of Amsterdam and Center for High-Energy Astrophysics, Amsterdam
Received 1990 April 23; accepted 1990 June 18

ABSTRACT

Radio observations of Sco X-1 were made on 1989 March 10–11 with the VLA, the WSRT, and the Australian Telescope as part of a multiwavelength campaign with the *Ginga* X-ray satellite, the *IUE* satellite, and other ground-based instruments. Two source states were detected in the radio and X-ray data, with Sco X-1 being "radio-quiet" when it was in the X-ray "flaring branch" and "radio-loud" when it was in the X-ray "normal branch," the same type of radio–X-ray correlation seen in the "Z-sources" GX 17+2 and Cyg X-2. Both radio-quiet and radio-loud states showed radio spectrum changes indicating a multicomponent radio source where the high-frequency component is variable on time scales of 2–3 hr.

Subject headings: stars: individual (Scorpius X-1) — stars: radio radiation — X-rays: binaries

I. INTRODUCTION

Sco X-1 was the first X-ray binary found to have a radio counterpart (Andrew and Purton 1968; Ables 1969; Hjellming and Wade 1971). It has both flaring radio emission on time scales of minutes to hours and an apparent double radio source with components located 1.″2 NNE and SSW (Hjellming and Wade 1971; Wade and Hjellming 1971). It was the first X-ray binary in which an X-ray flare was observed (Lewin, Clark, and Smith 1968) and the first one subjected to extensive, multiwavelength observing campaigns (Canizares *et al.* 1973; Bradt *et al.* 1975). These led to the suggestion that its "radio-loud" and "radio-quiet" states were related to certain states of the X-ray source (Priedhorsky *et al.* 1986). Sco X-1 is now identified as one of the six "Z-sources"—low-mass X-ray binaries with three identifiable X-ray states associated with a "Z-like" X-ray "color-color" plot (Hasinger and van der Klis 1990). Recent multiwavelength observations, involving the Very Large Array (VLA) and the *Ginga* X-ray satellite, of two other "Z-sources," GX 17+2 and Cyg X-2, showed that state changes in the X-ray source are directly associated with changes in the state of the radio emission (Penninx *et al.* 1988; Hjellming *et al.* 1990). This paper reports on VLA, Westerbork Synthesis Radio Telescope (WSRT), and Australian Telescope (AT) radio observations and *Ginga* X-ray observations of Sco X-1 on 1989 March 10–11 during another multiwavelength campaign involving these instruments, the *IUE* satellite, and other ground-based telescopes. Sco X-1 was observed in both "flaring" and "normal" branch X-ray states and the associated radio emission was "radio-quiet" and "radio-loud," respectively, following the same behavior pattern previously seen for GX 17+2 and Cyg X-2.

[1] The National Radio Astronomy Observatory is operated by Associated Universities, Inc., under a cooperative agreement with the National Science Foundation.

II. THE VLA, WSRT, AND AT RADIO OBSERVATIONS

The VLA observations of Sco X-1 were made at frequencies of 1.49, 4.9, and 8.4 GHz between 8:30 and 16:30 UT on 1989 March 10 and between 7:58 and 10:25 on 1989 March 11. The VLA was in its 10 km B-array during the observations. The variable radio component coincident with Sco X-1 was determined by subtracting from the observed visibilities the visibilities for the other sources in the field. Because Sco X-1 was relatively weak on the first day, and the observations covered a wide range of hour angles, the models for the non–Sco X-1 visibilities were determined as a byproduct of obtaining CLEANed images, with the CLEAN components everywhere except at the position of Sco X-1 constituting the model. The results are listed in Table 1 and plotted in Figure 1. Sco X-1 was relatively weak and slightly variable on March 10; however it was stronger and had a wider range of variability on March 11.

The Australian Telescope radio observations of Sco X-1 were made from 14:15 UT March 10 to 0:44 UT March 11, using two elements of the telescope operating at 8.73 GHz. Unfortunately, because so few telescopes were available, since it was early in the construction phase of the AT, only upper

TABLE 1

1989 MARCH 10–11 VLA RADIO DATA FOR SCO X-1

JD −2,440,000.5	UT (Start)	UT (Stop)	$S_{4.9}$ (mJy)	$S_{4.9}$ (mJy)	$S_{8.4}$ (mJy)	Error (mJy)
7596.361	8:30:40	8:49:00		1.09		±0.1
7596.374	8:56:10	9:01:20	2.72			±0.2
7596.378	9:01:30	9:07:20		1.18		±0.12
7596.382	9:07:30	9:13:20			0.3	±0.1
7596.391	9:16:40	9:29:50		1.09		±0.1
7596.403	9:37:10	9:43:20	2.66			±0.19
7596.408	9:43:30	9:49:50		1.11		±0.11
7596.412	9:50:00	9:56:10			0.63	±0.09
7596.423	9:59:30	10:17:40		1.29		±0.09
7596.437	10:25:00	10:33:10	2.78			±0.16
7596.443	10:33:20	10:40:40		1.23		±0.1
7596.448	10:40:50	10:49:10			0.81	±0.8
7596.46	10:52:20	11:11:30		1.28		±0.09
7596.473	11:19:00	11:23:00	3.04			±0.21
7596.476	11:23:10	11:28:00		1.38		±0.11
7596.48	11:28:10	11:33:00			0.62	±0.09
7596.488	11:36:30	11:49:30		1.43		±0.09
7596.5	11:56:50	12:05:50	3.11			±0.17
7596.507	12:06:00	12:14:50		1.09		±0.1
7596.514	12:15:00	12:24:50			0.89	±0.08
7596.527	12:28:20	12:49:20		1.34		±0.08
7596.542	12:56:30	13:04:10	2.62			±0.16
7596.548	13:04:20	13:12:40		1.49		±0.1
7596.554	13:12:50	13:21:10			1.39	±0.08
7596.564	13:28:30	13:36:10	2.47			±0.16
7596.57	13:36:20	13:44:40		1.5		±0.1
7596.576	13:45:00	13:53:10			0.77	±0.09
7596.586	14:00:30	14:08:00	2.29			±0.17
7596.592	14:08:10	14:16:30		1.46		±0.1
7596.598	14:16:50	14:25:00			0.85	±0.09
7596.608	14:32:40	14:39:30	1.94			±0.19
7596.614	14:39:50	14:47:40		1.43		±0.1
7596.62	14:48:30	14:55:20			1.24	±0.1
7596.63	15:03:00	15:09:50	2.47			±0.2
7596.635	15:10:10	15:17:50		1.89		±0.11
7596.641	15:19:00	15:26:00			2.01	±0.1
7596.651	15:33:30	15:40:20	2.32			±0.2
7596.656	15:40:30	15:47:20		1.90		±0.11
7596.661	15:47:30	15:55:20			1.55	±0.1
7596.669	15:58:50	16:07:40		1.84		±0.1
7596.676	16:07:50	16:17:50	2.77			±0.2
7596.683	16:18:00	16:27:50			0.97	±0.1
7597.342	8:09:50	8:16:00	9.9			±0.25
7597.347	8:16:20	8:22:00			6.8	±0.2
7597.352	8:23:10	8:30:10		8.2		±0.2
7597.357	8:30:10	8:38:10		6.2		±0.2
7597.363	8:38:10	8:46:10		6.8		±0.2
7597.37	8:49:20	8:55:00	8.5			±0.25
7597.374	8:55:10	9:02:30			4.3	±0.15
7597.384	9:09:50	9:16:50		6.0		±0.15
7597.39	9:17:00	9:24:50	8.7			±0.2
7597.395	9:25:00	9:32:20			3.5	±0.15
7597.405	9:39:40	9:46:50		5.7		±0.15
7597.411	9:47:00	9:54:50	7.7			±0.15
7597.416	9:55:00	10:02:20			5.4	±0.15
7597.426	10:09:40	10:16:40		5.8		±0.15
7597.431	10:16:50	10:24:50	8.2			±0.15

limits were obtained as shown in Table 2, all at levels considerably above the Sco X-1 radio fluxes observed with the VLA.

The WSRT observed Sco X-1 at 90 cm on 1989 March 11 between 0000 and 0900 UT. The upper limit for the average flux during this period was 15 mJy.

III. COMPARISON OF RADIO AND X-RAY STATES IN SCO X-1

In Figure 1 we plot the VLA radio fluxes of Sco X-1 at 1.49 (*filled circles*), 4.9 (filled triangles), and 8.4 GHz (X's) as a function of modified Julian Date (=JD −2,440,000.5). The solid curves are least-squares fits to polynomials that reflect the significant changes in the data at each frequency on 1989 March 10 and 11, respectively. These data indicate a multicomponent radio source, with one component which is most variable at higher frequencies.

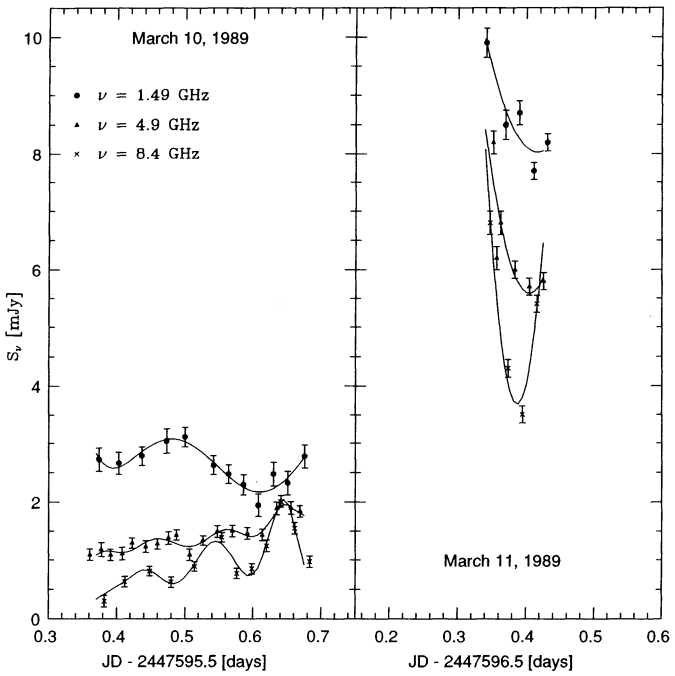

FIG. 1.—VLA radio flux density variations of Sco X-1 on 1989 March 10 and 11 (1.49 GHz, *filled circles*; 4.9 GHz, *filled triangles*; 8.4 GHz, X's) with polynomial fits reflecting the significant variations of the data.

In Figure 2*a* the radio data are plotted on a scale that can be compared with the X-ray "hardness," $H_2 = I(3.5\text{–}5.8\ \text{keV})/I(1.2\text{–}3.5\ \text{keV})$ measured with *Ginga*. The X-ray data are discussed in detail in separate papers concentrating on the X-ray results for the Sco X-1 campaign (Wood *et al.* 1989; Hertz *et al.* 1990). The X-ray "hardness," H_2, measured with the *Ginga* X-ray satellite is plotted as a function of modified Julian Day in Figure 2*b*. As identified at the top of Figure 2*b*, Sco X-1 was in a "flaring branch" X-ray state before 7596.1 and in a "normal branch" X-ray state after that time.

TABLE 2

1989 MARCH 10 AUSTRALIAN RADIO TELESCOPE DATA FOR SCORPIUS X-1

UT (Start)	UT (Stop)	$S_{8.73}$ (mJy)
1415.....	1425	$<13 \pm 5$
1510.....	1520	$<20 \pm 5$
1545.....	1555	$<22 \pm 5$
1618.....	1627	$<26 \pm 5$
1640.....	1659	$<17 \pm 3$
1720.....	1730	$<24 \pm 4$
1753.....	1803	$<45 \pm 4$
1954.....	2004	$<33 \pm 3$
2024.....	2044	$<28 \pm 3$
2225.....	2235	$<24 \pm 4$
2305.....	2315	$<37 \pm 4$
2340.....	2350	$<20 \pm 5$
2434.....	2444	$<15 \pm 5$

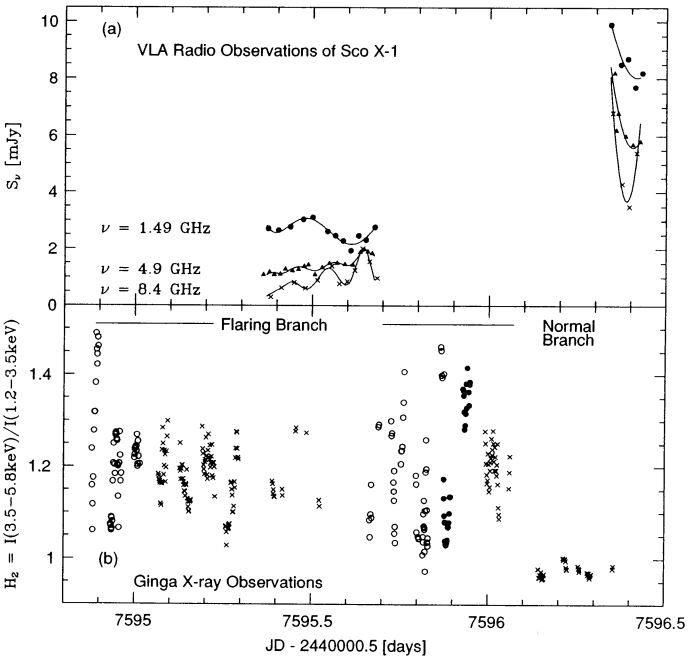

FIG. 2.—(*a*) VLA radio flux density data on Sco X-1 (1.49 GHz, *filled circles*; 4.9 GHz, *filled triangles*; 8.4 GHz, X's) for 1989 March 10 and 11 with polynomial fits to the data and (*b*) *Ginga* X-ray hardness measurements of Sco X-1 made 1989 March 9–11 (with three different instrumental configurations indicated by X's, filled, and open circles as discussed in the text) are plotted as a function of Julian Day −2,440,000.5, with identification of "flaring" branch states on March 10 and "normal" branch states on March 11.

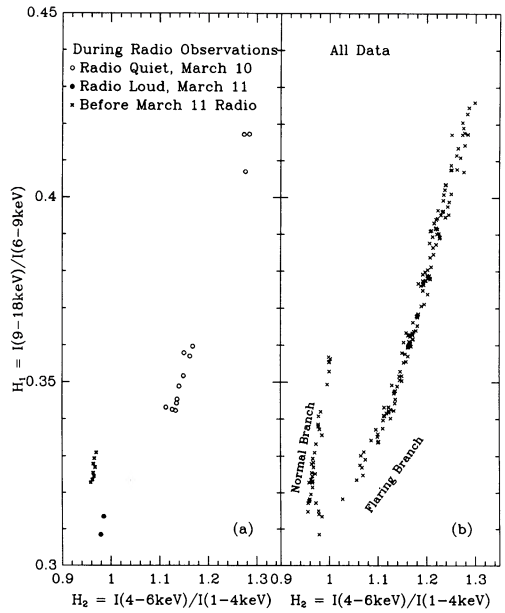

FIG. 3.—X-ray "color-color" plots in the form of $H_1 = I(9–18\text{ keV})/I(6–9\text{ keV})$ vs. $H_2 = I(4–6\text{ keV})/I(1–4\text{ keV})$ are plotted for (*a*) periods with simultaneous radio observations (*filled circles*), or just minutes before the radio observations (X's), for the "radio-loud" state and open circles for the "radio-quiet" state; and (*b*) all X-ray "flaring" and "normal" branch data (X's).

The *Ginga* X-ray observations were made with three different instrumental configurations, each with different combinations of time and spectral resolution. The ratios of intensities used to determine X-ray hardness for the different configurations differ only by constant scale factors. Therefore, in order to plot comparable values of X-ray hardness in Figures 2*b* we have scaled the hardness for two of these configurations (*open and filled circles*) so the mean during the "flaring branch" observations has the same value as the mean for the unscaled hardness (X's) during this period. The nearly continuous variation of hardness on short time scales before 7596.1 is one of the principal characteristics of flaring branch states. This is contrasted with the lower hardness level, and lack of short time scale hardness variations after 7596.1 when the source was in a normal branch state.

The radio observations shown in Figure 2*a* indicate two levels of Sco X-1 radio fluxes which one can call "radio-quiet" (March 10) and "radio-loud" (March 11). Comparison of Figures 2*a* and 2*b* show that the radio-quiet state corresponded to the flaring branch X-ray states and the radio-loud state corresponded to the normal branch X-ray states. Figure 3*a* shows "color-color" plots, H_1 [$= I(9–18$ kev$)/I(5.8$ keV$)$] versus H_2, for the X-ray data at or near the time radio observations were made, with open circles corresponding to the X-ray flaring branch states and filled circles and X's identifying normal branch states. Figure 3*b* shows a plot of the same quantities for all times of X-ray observations. Figure 3 incorporates only *Ginga* data from the same instrumental configuration (X's in Fig. 1*b*).

The importance of the radio-loud versus radio-quiet behavior of Sco X-1, even with sampling of only two X-ray states, is that it is consistent with the radio–X-ray coupling in GX 17+2 (Penninx *et al.* 1988) and Cyg X-2 (Hjellming *et al.* 1990). Radio emission is weakest when the X-ray source is in the flaring branch, stronger when in the normal branch, and strongest of all when in the horizontal branch sampled in the GX 17+2 and Cyg X-2 observations.

The continuous radio sampling of flaring branch states in Sco X-1 for a period of 8 hr on March 10 was, unfortunately, the period of sparsest X-ray sampling (cf. Fig. 2*b*). Complex radio source evolution, with variations by a factor of 1.5 at 1.49 GHz and a factor of 4 at 8.4 GHz occurred during this period. The time variation curves, obtained from polynomial fits to the data for each radio frequency in Figure 1, indicate the significant variations.

On March 10 there were three significant peaks of "events" at 8.4 GHz that are related to slightly delayed or simultaneous peaks at 4.9 GHz, with spectral index varying from $\alpha \sim -1.1$ ($S_\nu \approx \nu^\alpha$) to values indicating a flatter spectral index, with $\alpha \sim 0$ near the second and third maxima in the two higher frequency curves. The three peaks are separated by intervals of $\sim$2.5 hr. The variations at 1.49 GHz are not obviously coupled to the higher frequency variations unless the late rise is a delayed reflection of the preceding overall flux increases in the high-frequency curves. The initial spectral index between 1.49 and 4.9 GHz is ~ -0.7 for the first half of the observed period, then increases to ~ -0.2 before decreasing to ~ -0.3 near the end.

The spectral evolution on March 11 reflects more extreme variations of at least two components of radio emission. The first data show a rapidly decaying radio source with a power-law spectrum with $\alpha \sim -0.2$, which then decayed more rapidly at the higher frequencies, producing a curved spectrum. However, a flaring event first seen at 8.4 GHz counteracts the decay and this event propagates with lesser amplitude to the lower frequencies.

The Sco X-1 radio data for both radio-"quiet" and radio-"loud" days are dominated by the mixture of the decay of a

curved spectrum component and the rise and decay of a component with spectrum peaking at $\nu \geq 8$ GHz. The rise and decay of the latter component take place on time scales of 2–3 hr. Because of lack of frequency resolution we cannot estimate the peak frequency for the two dominant components, but it is clear that the high-frequency component is smaller and more variable than the other component. The dominant negative spectral indices and the tendency for flaring events to be stronger at the higher frequencies, with delays in the peaks at lower frequencies, are indicative of multiple synchrotron radiation "events" with adiabatically expanding components (Hjellming and Johnston 1988).

IV. ANALYSIS OF RADIO SOURCE VARIATIONS

While the radio source variations plotted in Figure 1 do not correspond to any simple model of a stable or evolving radio source, because there are at least two components with different size and time scales dominating the lower and higher radio frequencies, there are a number of conclusions that can be derived from the observations. First of all, there are time variations on time scales of $\sim$40 minutes. From this we can estimate the size of the emitting regions to be less than or equal to 6×10^{13} cm if the radio emission is assumed to be incoherent. Assuming a distance of 500 pc, this corresponds to a geometric mean size scale less than or equal to 0.01 arcseconds, a solid angle of $\theta_1\theta_2 \leq (0''.1)^2$, and a brightness temperature $T_b \geq 8 \times 10^6 S_\nu(\text{mJy}) \times (\lambda_{\text{cm}}/20)^2$ K. With flux densities above 10 mJy: this implies brightness temperatures greater than or equal to 10^8 K. This fact, the nonthermal radio spectral indices, and the time scale of variation indicate the radio emission is due to compact synchrotron-radiating regions of mixed relativistic electrons and magnetic fields. Comparable radio source behavior in Cyg X-2 and GX 17+2, which are much more distant, indicate comparable size scales and much higher brightness temperatures.

Having three frequency variations of a synchrotron radio source allows us to make further estimates of source parameters. While the radio emission regions may be very complex, let us assume that at any time t the radio emitting regions have an average depth L, a solid angle $\theta_1\theta_2 = \theta_0^2$, an average magnetic field H, and a power-law relativistic electron number density proportional to $KE^{-\gamma}$. Under these circumstances (Hjellming and Johnston 1988)

$$S_\nu = (j_0/\kappa_0)\theta_1\theta_2(\nu/\nu_0)^{5/2}[1 - e^{-\kappa_0 L(\nu/\nu_0)^{-(\gamma+4)/2}}] , \quad (1)$$

where

$$j_0/\kappa_0 = 2.73 \times 10^{-30}[a(\gamma)/g(\gamma)] \times H^{-1/2} \times \nu_0^{5/2}/2^{\gamma/2} \quad (2)$$

and

$$\kappa_0 = 0.019 g(\gamma) \times (3.6 \times 10^9)^\gamma \times K \times H^{(\gamma+2)/2} \times \nu_0^{-(\gamma+4)/2} \quad (3)$$

where $a(\gamma)$ and $g(\gamma)$ are slowly varying functions that are the order of unity.

The curved spectra at different stages of the observations can be used to solve for certain parameter combinations in equations (1)–(3). With $S_0 = (j_0/\kappa_0)\theta_1\theta_2$ and $\tau_0 = \kappa_0 L$ at $\nu_0 = 4.9 \times 10^9$ GHz, the curved spectra at two epochs early on March 10, and two epochs early on March 11, are fitted by $S_0 = 57$, 73, 250, and 260 mJy; $\tau_0 = 0.02$, 0.02, 0.022, and 0.025; and $\gamma = 5.3$, 2.54, 2.51, and 2.25. The two parameters that can then be determined from S_0 and τ_0 are the brightness temperature ($T_0 = \lambda_0^2 \times (j_0/\kappa_0)/(2k)$), where k is the Boltzmann constant) and $\theta_0/H^{1/4}$. The latter for the four epochs is found to be 0.38, 0.20, 0.36, and 0.34 milliarcseconds per gauss$^{1/4}$, and the corresponding brightness temperature at 6 cm is 7.2×10^9, 3.5×10^{10}, 3.5×10^{10}, and 4.1×10^{10} K. While one must be careful about assuming equipartition of energy between relativistic electrons and magnetic fields under time variable conditions, these results and that assumption would lead to an estimate of $H \sim 10^{-3}$–10^{-4} gauss, which is a typical result for X-ray binary radio emission. This then indicates a source size of $\sim$0.03 milliarcseconds, which for a distance of 500 pc corresponds to a size scale estimate $\sim 2 \times 10^{11}$ cm.

V. CONCLUSIONS

Sco X-1 is the third of the so-called "Z-sources," which have well defined X-ray hardness–hardness diagrams that identify the state of the X-ray emission of an X-ray binary, to be observed with coupled X-ray and radio states. Observed only in the X-ray "normal" and "flaring" branch states, Sco X-1's behavior is consistent with the results for GX 17+2 (Penninx *et al.* 1988) and Cyg X-2 (Hjellming *et al.* 1990) in that its radio emission is weakest and least variable during the flaring branch state, and strongest and most variable while in a normal branch state. The three frequency, long time scale observations of Sco X-1 show for the first time that during both flaring and normal branch states there are at least two separate radio emission components, one with a peak near 1 GHz and another with a peak greater than or equal to 8 GHz.

The radio emission for Sco X-1 varies on time scales as short as 40 minutes, and this fact, coupled with source size estimates of $\sim 2 \times 10^{11}$ cm and the conservative assumption that the radio emission is incoherent synchrotron radiation, implies propagation velocities greater than or equal to $0.003c$ for the effects of a change in the X-ray–emitting accretion environment propagating out to the radio-emitting regions. Another possibility that cannot be excluded by the observations is that the radio emission is partially coherent and hence much smaller, in which case it could be due to ejection of relativistic electrons from a magnetized neutron star in a "cocooned" pulsar scenario (Hjellming *et al.* 1990). The implied "jet" or cocooned pulsar options are just varying degrees in which radio emission arises from energetic ejecta that is highly coupled to changes in the accretion disk environment.

REFERENCES

Ables, J. G. 1969, *Ap. J. (Letters)*, **155**, L27.
Andrew, B. H., and Purton, C. H. 1968, *Nature*, **218**, 855.
Bradt, H. V., *et al.* 1975, *Ap. J.*, **197**, 443.
Canizares, C. R., *et al.* 1973, *Ap. J. (Letters)*, **179**, L1.
Hasinger, G., and van der Klis, M. 1990, *Astr. Ap.*, in press.
Hertz, P., Norris, J. P., Wood, K. S., Michelson, P. F., Vaughn, B. A., Dotani, T., and Mitsuda, K. 1990, in preparation.
Hjellming, R. M., and Johnston, K. J. 1988, *Ap. J.*, **328**, 600.

Hjellming, R. M., and Wade, C. M. 1971, *Ap. J. (Letters)*, **164**, L1.
Hjellming, R. M., Han, X., Cordova, F. A., and Hasinger, G. 1990, *Astr. Ap.*, **235**, 147.
Lewin, W. H. G., Clark, G., and Smith, W. B. 1968, *Ap. J. (Letters)*, **152**, L55.
Penninx, W., *et al.* 1988, *Nature*, **336**, 146.
Priedhorsky, W., *et al.* 1986, *Ap. J. (Letters)*, **306**, L91.
Wade, C. M., and Hjellming, R. M. 1971, *Ap. J.*, **170**, 523.
Wood, K. S., Hertz, P., Norris, J. P., Vaughan, B. A., Michelson, P. F., Kitsuda, K., and Dotani, T. 1989, in *Proc. 23rd ESLAB Symp. on Two Topics in X-Ray Astronomy*, ed. J. Hunt and B. Batrick (ESA Publications: Noordwijk), Vol. **1**, p. 689.

P. HERTZ, J. P. NORRIS, and K. S. WOOD: E. O. Hulburt Center for Space Astronomy, Naval Research Laboratory, Washington, DC 20375-5000

R. M. HJELLMING: NRAO, P.O. Box O, Socorro, NM 87801-0387

K. MITSUDA: Institute of Space and Aeronautical Science, 3-1-1 Yoshinodai, Sagamihara-shi, Kanagawa-ken, 229 Japan

W. PENNINX and J. VAN PARADIJS: Astronomical Institute "Anton Pannekoek," University of Amsterdam, Roetersstraat 15, 1018 WB Amsterdam, The Netherlands

R. T. STEWART and G. L. WHITE: CSIRO, Division of Radio Physics, P.O. Box 76, Epping, NSW, Australia

R. STROM: Netherlands Foundation for Research in Radio Astronomy, Radiosterrenwacht, P.O. Box 2, 7990 AA Dwingeloo, The Netherlands